Research Square

Preprints are preliminary reports that have not undergone peer review.
They should not be considered conclusive, used to inform clinical practice,
or referenced by the media as validated information.

Pathways towards climate and health co-benefits in global ruminant sector

Shuai Ren

shuairen707@gmail.com

Massachusetts Institute of Technology https://orcid.org/0000-0002-6190-755X

Yingfang Cao

Northwest Institute of Plateau Biology, Chinese Academy of Sciences

Qing Hu

Beijing Municipal Ecological and Environmental Monitoring Center

Robert Powell

Department of Plant Sciences, University of Cambridge

Michael Windisch

Department of Environmental Systems Science, ETH Zurich

Yi Xi

Laboratoire des Sciences du Climat et de l'Environnement https://orcid.org/0000-0003-2654-4615

Xuejun Liu

China Agricultural University https://orcid.org/0000-0002-8367-5833

Adam Pellegrini

University of Cambridge https://orcid.org/0000-0003-0418-4129

César Terrer

Massachusetts Institute Of Technology https://orcid.org/0000-0002-5479-3486

Biological Sciences - Article

Keywords:

Posted Date: June 27th, 2025

DOI: https://doi.org/10.21203/rs.3.rs-6849384/v1

License: This work is licensed under a Creative Commons Attribution 4.0 International License.
Read Full License

Additional Declarations: There is **NO** Competing Interest.

Pathways towards climate and health co-benefits in global ruminant sector

Shuai Ren[1]*, Yingfang Cao[2], Qing Hu[3], Robert S. Powell[4], Michael G. Windisch[5], Yi Xi[6], Xuejun Liu[7], Adam F. A. Pellegrini[4], César Terrer[1]

[1]Department of Civil and Environmental Engineering, Massachusetts Institute of Technology, Cambridge, MA, USA

[2]Qinghai Provincial Key Laboratory of Restoration Ecology for Cold Region, Northwest Institute of Plateau Biology, Chinese Academy of Sciences, Xining, China

[3]Beijing Municipal Ecological and Environmental Monitoring Center, Beijing, China

[4]Department of Plant Sciences, University of Cambridge, Cambridge, UK

[5]Institute for Atmospheric and Climate Science, Department of Environmental Systems Science, ETH Zurich, Zurich, Switzerland

[6]Laboratoire des Sciences du Climat et de l'Environnement, LSCE/IPSL, CEA-CNRS-UVSQ, Université Paris-Saclay, Gif-sur-Yvette, France

[7]State Laboratory of Nutrient Use and Management, College of Resources and Environmental Sciences, China Agricultural University, Beijing, China

*Correspondence to shuairen707@gmail.com

The global ruminant sector is a major source of greenhouse gas (GHG) emissions and a key provider of human nutrition. Yet, reconciling its environmental impacts with nutritional needs remains a critical challenge. Here, we first present a comprehensive, system-level global assessment of GHG emissions from the ruminant sector. We estimate that about 1,060 Gt CO_2-eq or 0.3 °C of warming has been caused globally between 1961 and 2019. Contrary to previously assumed, land-based emissions resulting from livestock grazing and deforestation are the main contributor, particularly in tropical regions. Without intervention, ruminant-related emissions are projected to triple by 2100. We find that while a shift towards more plant-based diets could yield substantial climate benefits, these are limited by potential health trade-offs. A synergistic strategy combining demand- and supply-side measures could reduce ruminant emissions by up to 91% by 2100 while meeting the nutritional requirements of a healthy diet, together leading to a 6.5% increase in global gross domestic product. Under this scenario, 71% of countries could achieve neutral or negative ruminant GHG emissions by 2100, though optimal strategies vary: tropical countries should prioritize land-based interventions, whereas others may benefit more from demand-side measures. Our findings call for a rapid, integrated transformation of the ruminant sector to alleviate the dual burden of meeting national climate and nutrition targets.

Main text

Agriculture is responsible for about 15% of anthropogenic warming[1], with greenhouse gas (GHG) emissions from the ruminant sector being a major contributor[2,3]. The ruminant sector encompasses a variety of GHG sources and sinks across both on-farm and off-farm stages (Fig. S1), yet a holistic, system-level assessment of these emissions is still lacking. This is because the existing approaches remain simplistic and may even overlook some important sources of emissions[4], particularly for land-based processes. For example, ongoing grazing activities, such as feeding and trampling, can alter plant photosynthesis[5], soil microbial activities[6], and land-atmosphere energy and water exchanges[7], thereby affecting GHG fluxes and local surface temperatures—yet these effects are rarely considered[4,8]. Likewise, land-use change emissions (e.g., pasture-driven deforestation) often rely on simplified Tier 1 methods from the Intergovernmental Panel on Climate Change (IPCC)[4,9,10], which might introduce substantial biases[11]. With a growing and more affluent population, global ruminant production is expected to increase in the future[12,13]. This underscores the need for comprehensive and disaggregated ruminant GHG assessments to better understand the climate impacts and inform effective strategies.

The ruminant sector offers considerable opportunities for climate mitigation[13,14]. Demand-side strategies, such as reducing ruminant meat consumption, are recognized as practical and effective in reducing GHG emissions[4,15,16]. However, a global shift towards more plant-based diets may pose nutritional challenges for human health, especially in poor countries[17,18]. In many low-income regions, animal-sourced foods are among the few affordable sources of high-quality protein, iodine, zinc and vitamin B_{12}[19]. Therefore, indiscriminate reductions in meat consumption could exacerbate undernutrition. To date, there is limited quantitative evidence on what level of meat reduction is most effective in balancing the trade-offs between climate and health outcomes. On the production side, smarter grazing management (e.g., optimizing stocking rates and pasture recovery) can cut soil emissions and, under some conditions, turn grasslands into net carbon sinks[11,20], yet these options are rarely considered in global assessments. How such producer-side measures interact with consumer-level ones remains poorly understood. Recent studies have provided insights into plausible pathways for reducing GHG emissions in sectors such as plastic waste[21], construction[22] and the pulp and paper industry[23]. Whether similarly tailored, country-specific pathways can drastically reduce GHG emissions from the ruminant sector while providing essential nutrition for human health remains unexplored.

Here, we provide a system-level analysis and roadmap aligning the global ruminant sector with both climate-mitigation and nutrition goals, leveraging an integrated framework that combines meta-analysis of 6,816 field-based monthly GHG and carbon sequestration measurements (Fig. S2), remote sensing datasets, machine learning, and life cycle assessment. First, we systematically quantified GHG emissions from the global ruminant sector between 1961 and 2019, and projected future emissions for 2020-2100 under a business-as-usual (BAU) scenario. Distinct from previous studies that primarily consider emissions from livestock and off-farm stages[4,8], our analysis additionally accounts for land-based emissions arising from ongoing grazing activities and pasture-driven deforestation (Fig. S1). Second, we translated these emissions into associated temperature increases and benchmark them against the remaining 1.5 °C and 2 °C carbon-budget targets from the Paris Agreement. Third, we evaluated the climate and health impacts of different levels of meat consumption and assessed the associated economic impacts in order to identify the most effective dietary transitions. Finally, we explored a range of demand- and supply-side strategies (including optimized grazing, zero deforestation, shifting to more optimistic population growth, improved production efficiency and halving food waste) to identify country-specific plans to drastically reduce ruminant emissions without compromising essential animal-source nutrients within a given dietary pathway.

Global GHG emissions from the ruminant sector

In this study, we quantified ruminant GHG emissions by establishing a sector-wide accounting boundary encompassing five key categories: ongoing grazing land, pasture-driven deforested land, abandoned agricultural land, live animals, and human consumption of animal products (post-farm gate emissions) (Fig. S1; see Methods for more details). Specifically, land-based emissions due to livestock grazing and deforestation account for both biogeochemical fluxes (BGC; CO_2, CH_4, and N_2O) and biogeophysical (BGP) effects on local temperatures.

From 1961 to 2019, the global ruminant sector cumulatively emitted about 1,060 ± 894 Gt CO_2-eq (Fig. 1; Table S1), which corresponds to an additional warming of 0.3 °C based on a carbon-climate response of 0.29 °C per thousand Gt CO_2 emitted[24]. In 2019, global GHG emissions from the ruminant sector were estimated as 22 ± 15 Gt CO_2-eq yr^{-1} (Fig. 1a), which is comparable to those from the entire global food system (18 Gt CO_2-eq yr^{-1})[10] and about 40% lower than global industrial GHG emissions (38 Gt CO_2-eq yr^{-1})[25]. Driven by rising

demand for animal products[13], the annual emissions increased by 70% from 1961 (13 Gt CO_2-eq yr^{-1}) to 2019 (22 Gt CO_2-eq yr^{-1}) (Fig. 1a), yet the ruminant sector's share in total anthropogenic GHG emissions has decreased from 41% to 32% (Fig. 1b) because other sectors rose even faster.

Contrary to our expectations, land-based GHG emissions, especially grazing-induced BGC CO_2, dominated the cumulative emissions from 1961 to 2019, accounting for 62% (Fig. 1c and Fig. S3). This exceeded the contributions from non-CO_2 emissions beyond the farm gate (22%) and from live animals (17%) (Fig. S3), which are commonly believed to be the dominant sources according to current understanding[4]. The highest grazing-induced CO_2 emissions occurred in tropical regions with intense grazing pressure and warm climates (Figs. S4-S5)[11], where plant carbon uptake was suppressed and soil CO_2 release accelerated[11].

Beyond the grazing-induced BGC emissions, contributions from deforestation, grazing-induced BGP and non-CO_2 emissions, and carbon uptake from abandoned agricultural land were smaller globally over this period (Fig. 1a and Fig. S3), but can be critical at local scales. For example, livestock grazing on wetlands could lead to substantial CH_4 emissions, which are about seven times higher than those of upland soils, particularly under heavy grazing pressure (Fig. S6). This highlights the importance of restoring degraded wetlands for climate mitigation[26]. Moreover, deforested areas for pasture covered only 1.5 Mkm^2 globally (4 % of total grazing lands), but their combined BGC and BGP contributions represented 7 % to total emissions during 1961–2019 (78 ± 100 Gt CO_2-eq; Table S1), reflecting their exceptionally high emission intensity per unit area (Figs. S7-S9). Previous studies have typically applied IPCC Tier 1 emission factors on a very coarse scale[4,8,10], instead of spatially-explicit emissions as we do here, underestimating emissions from deforestation by a factor of three (Fig. S10a), especially in Brazil and China (Fig. S10b).

There are substantial regional variations in the long-term trends, cumulative amounts, and sectoral composition of the GHG emissions. From 1961 to 2019, annual emissions showed increasing trends across the world, with the most rapid increases observed in Western Asia and Northern Africa (58%) and China (38%) (Fig. S11a). In contrast, annual per capita emissions declined for most regions or countries especially in Oceania and Sub-Saharan Africa (Fig. S11b). The global hotspots of cumulative GHG emissions are located in South and North America, eastern Asia, and Oceania (Fig. 2a). Sub-Saharan Africa and South America were among the largest contributors, together accounting for 56% of global emissions or producing approximately 595 Gt CO_2-eq over 1961-2019—of which 84% came

from land-based sources (Fig. 2c and Fig. S4). At the national level, Brazil had the highest total GHG emissions (~195 Gt CO_2-eq), primarily driven by grazing and deforestation (Fig. 2c). Together with the United States, Australia, China, and India, the top five countries emitted about 484 Gt CO_2-eq—six times more than Europe, which mainly came from the consumption of livestock products (Fig. 2c). Although tropical countries show relatively high ruminant-related emissions, it is important to recognize that a substantial share of the emissions may not be solely attributable to domestic consumption but could also be driven by trade-oriented livestock demand. Accounting for trade-adjusted emissions would provide deeper insights into national responsibility.

Based on historical consumption patterns and socioeconomic indicators (e.g., income and trade; see Methods), we forecasted BAU emissions from the global ruminant sector, which served as the baseline scenario. Our analysis showed that, without human interventions, the global ruminant sector is expected to generate an estimated 2,961 ± 1,508 Gt CO_2-eq over the next eighty years (Fig. 1c; Table S1), nearly tripling the cumulative emissions observed over the past sixty years (Fig. 1c). To meet the warming targets of the Paris Agreement with a 50% probability, the maximum global GHG emissions allowed by 2100 are estimated to be 705 Gt CO_2-eq for 1.5°C warming and 1,816 Gt CO_2-eq for 2°C warming[27]. In this case, our BAU ruminant estimates of 2,961 Gt CO_2-eq overshoots both climate targets by 320% and 63%. We predicted that annual ruminant emissions will reach 51 ± 17 Gt CO_2-eq yr^{-1} in 2100, an increase of almost 300% from 1961 levels (13 Gt CO_2-eq yr-1) (Fig. 1a), and remain dominated by land-based fluxes in tropical nations (Fig. 2b, d and Figs. S4, S8, S12).

Climate and health trade-offs under global meat reduction

Overall, the previous section underscores the urgency of reducing ruminant-related emissions. While earlier studies have demonstrated the substantial climate benefits of reducing ruminant meat consumption, it is also important to consider the potential consequences for human health[17,18]. To evaluate which level of meat reduction would yield the greatest combined climate and health benefits, we translated both effects into a common economic metric. Avoided ruminant CO_2-equivalent emissions were valued using the social cost of carbon, while health impacts were monetized by converting changes in mortality (driven by shifts in the prevalence of underweight, overweight, and obesity) into economic terms using country-specific values of a statistical life (see Methods). Notably, the estimated economic costs and benefits are not an outcome of a sophisticated economic equilibrium

168 modelling effort[28], but only consider carbon costs and health effects on GDP.

169 The global net economic benefit (summing the climate and health components) of cutting
170 meat consumption increased with deeper cuts, peaked at ~70 % below BAU, and then
171 decreased (Fig. 3a). This pattern reflects divergent component responses. Consistent with
172 previous findings[15], greater meat reductions always shrink ruminant GHG emissions (Fig. 3a).
173 Health-related economic benefits initially increased and peaked at around a 70% reduction,
174 largely due to reduced mortality from overweight and obesity in rich countries consuming less
175 meat (Fig. S13). However, health benefits reversed once underweight mortality rises in low-
176 income countries (Fig. S13). At a 90 % reduction in meat consumption, health losses
177 outweigh climate gains, yielding a global benefit loss compared to the 70% reduction
178 scenario. These results imply that the climate benefit of very deep cuts may be partly offset by
179 health costs, a nuance sometimes overlooked in earlier global estimates[15].

180 Notably, our analysis has several limitations, mainly due to the exclusion of net carbon
181 sequestration from spared agricultural land and uncertainties in estimating health benefits the
182 spread in body mass index–mortality functions (Supplementary Text). To strengthen the
183 robustness of our conclusions, we further evaluated the climate and health benefits of two
184 unique dietary scenarios: the flexitarian EAT-Lancet "healthy diet"[29] and a strict vegan diet
185 (see Methods).

186 In line with previous studies[30,31], our analysis showed that a global shift from current
187 dietary patterns to the EAT-Lancet healthy diet could substantially reduce ruminant GHG
188 emissions from 2,961 Gt CO_2-eq to 1,767 Gt CO_2-eq over 2020–2100 (Fig. 3b). In a scenario
189 representing a global shift to a vegan diet, ruminant-sector emissions turn negative (i.e. the
190 freed land becomes a sink), removing (rather than emitting) from the atmosphere ~975 ± 385
191 Gt CO_2-eq over the next eighty years (Table S2). The largest contributions to this potential
192 come from forest biomass recovery on abandoned pasturelands (411 ± 90 Gt CO_2-eq) and
193 belowground carbon accumulation on rangelands (324 ± 372 Gt CO_2-eq) (Table S2). This
194 result highlights the strong climate benefit of completely eliminating meat consumption.
195 However, these climate benefits can be partly offset by the increased risk of underweight-
196 related mortality could offset much of the GHG gains (Fig. S14), resulting in a lower net
197 economic benefit (4.4 % of GDP) compared to the EAT-Lancet health diet (5 % of GDP) (Fig.
198 3c and Fig. S15; Supplementary Text). Notably, despite the clear climate benefits of a vegan
199 diet, the EAT-Lancet diet reduces ruminant-related GHG emissions by 40% over BAU,
200 enough to be in line with the emissions allowed to meet the 2 °C warming with a 50%

probability (Fig. 3b), but above emissions to meet the 1.5 °C target. These results highlight the need for more ambitious changes in the ruminant sector to bring it in line with global warming goals.

Strategies towards ruminant GHG mitigation

We next explored how global GHG emissions from the ruminant sector could be further reduced under the EAT-Lancet healthy diet by implementing six additional measures from the supply and demand sides (see Methods), including: (1) shifting population growth towards a more optimistic scenario (SSP1); (2) halving food waste and loss; (3) improving production efficiency of animal products; (4) avoiding deforestation for pasture expansion; (5) adjusting grazing intensity to the optimal level, which is derived from recent observational estimates[11] and (6) sparing land for carbon sequestration. We also assessed the potential GHG reductions achieved through some or all combinations of these strategies, resulting in a total of 48 different scenarios (Fig. 4a). In this section, we used the scenario involving only healthy dietary changes (BAU_{health}) as the baseline for comparison.

Our analysis showed that ruminant GHG emissions over 2020–2100 could be reduced by 4%–85% compared to the BAU_{health} (Fig. 4a), depending on the strategies implemented. In general, single-strategy scenarios achieve much smaller emission reductions than scenarios combining multiple strategies (Fig. 4a). For example, reducing food waste and loss—widely recognized as an effective mitigation option[32,33]—can result in a 12% reduction relative to BAU_{health} in our analysis. In contrast, combining this strategy with two additional demand-side measures doubled the ruminant GHG reduction to 24% (Fig. 4a). Notably, despite these opportunities, our analysis suggests that meeting the Paris Agreement targets remains difficult without incorporating strategies for land use and land cover change (Fig. 4b). In scenarios that include grazing management, more than half achieved cumulative emissions below the 1.5°C-compatible threshold, estimated at 705 Gt CO_2-eq for a 50% probability[27] (Fig. 4b). We observed that combining those strategies synergistically would reduce ruminant emissions by 85% compared to BAU_{health} (Fig. 4b) (hereafter the 'synergistic scenario'). Grazing management, such as optimizing grazing intensity based on recent observational estimates[11] and sparing agricultural land (including both pasture land or cropland used to feed livestock), emerged as the dominant contributor, accounting for 54% of the total mitigation potential (Fig. 4c). This was followed by preventing deforestation (17%) and reducing food waste and loss (15%), while improving production efficiency (9%) and lowing population growth rate

(5%) contributed the least (Fig. 4c).

Assuming immediate adoption of all studied strategies, total emissions from global ruminant sector would be only 263 Gt CO_2-eq over 2020-2100 under the synergistic scenario (Fig. 4), a 91% reduction compared to the BAU (2,961 Gt CO_2-eq; Fig. 1c). This level of emissions remains well within the maximum allowable budget, consistent with the Paris Agreement targets (Fig. 3b). Under this scenario, the remaining allowable emissions for the non-ruminant sectors would be recalculated as 442 Gt CO_2-eq and 1,553 Gt CO_2-eq to meet the 1.5°C and 2°C targets with a 50% probability, respectively, equivalent to about 12-42 years of current global industrial emissions[34]. Moreover, we found that implementation of all those strategies discussed could save about 13 Mkm^2 or 42% of global grazing land (Fig. S16), allowing an uptake of 402 Gt CO_2-eq in vegetation and soils by 2100 (Fig. S17a). This carbon removal could largely offset the emissions associated with live animals (416 Gt CO_2-eq), animal products (206 Gt CO_2-eq) and grazing land (43 Gt CO_2-eq) (Fig. S17a).

Regional differentiation in strategy contributions

There are substantial spatial variations in ruminant GHG emissions under the synergistic scenario (Fig. 5a). After global adoption of all six measures, 59 % of countries reach net-zero and a further 12 % become net-negative for 2020–2100, whereas the remaining 29 % still emit carbon (Fig. 5b). Countries with net emissions are mainly concentrated in developing regions such as South Asia (e.g., India; 139 Gt CO_2-eq), Sub-Saharan Africa (127 Gt CO_2-eq), and Western Asia and Northern Africa (23 Gt CO_2-eq) (Fig. S17b), where a substantial share of the global population lives. Feeding these large populations with healthy diets would inevitably result in considerable GHG emissions[31], posing significant challenges for these regions to achieve carbon neutrality for ruminant sector. Moreover, in other regions, carbon uptake from spared land or optimized grazing management could offset or even exceed the relatively low ruminant emissions, resulting in net-zero emissions (e.g., USA, Europe, and Brazil) or even net-negative emissions (e.g., Australia, rest of Central and Southern Asia, and Central and South Asia) (Fig. S17b). Nevertheless, our results showed that when compared to the BAU scenario, the largest absolute GHG reductions occur in Sub-Saharan Africa and South America, with savings of about 880 Gt CO_2-eq and 709 Gt CO_2-eq, respectively (Fig. S18).

The extent to which each strategy contributes to the mitigation potential under the synergistic scenario varies greatly by region (Fig. 5c). In Sub-Saharan Africa, South America

and Oceania, grazing management and avoiding deforestation are the main contributors (Fig. 5c). By contrast, demand-side strategies, including reducing food waste and loss and improving production efficiency, dominate in Europe, Canada, Western Asia and Northern Africa and South Asia. We found that in China and the United States, the relative importance of these strategies is more evenly distributed. Notably, shifting population growth towards a more optimistic scenario offers limited mitigation potential in most countries, with the exception of India, where it plays a crucial role (Fig. 5c). These findings highlight the need to carefully tailor strategies to specific regional contexts in order to maximize their climate effectiveness while protecting human health.

We estimate that transitioning from the BAU to the synergistic scenario would yield a global GDP gain of 6.5 % (Fig. 5d). The largest economic benefits are observed in Brazil (22 % of GDP), sub-Saharan Africa (13 % of GDP), and Oceania (12 % of GDP) (Fig. 5d), primarily driven by reductions in GHG emissions. Notably, the spatial distribution of GHG-related and health-related economic benefits differs: climate-related gains are concentrated in tropical countries, whereas health-related gains are more pronounced in mid- to high-latitude countries (Fig. S19).

Implication for targeted action

Adopting a system perspective, this study systematically assessed the GHG emissions within the global ruminant sector and identified potential pathways to deliver simultaneous climate and human health benefits. Particular emphasis was placed on addressing critical knowledge gaps on land-based emissions and mitigation opportunities using data-driven approaches.

Our results reveal that the global ruminant sector is a larger source of GHG emissions than previously recognized[2], generating approximately 1,060 Gt CO_2-eq between 1961 and 2019. Land-based biogeochemical and biogeophysical processes, which are often overlooked or simplified in previous studies[4,8], are the dominant contributors especially in tropical regions. This result challenges the widely held belief that non-CO_2 emissions from livestock (e.g., enteric fermentation) are the main driver[4], emphasizing the need for better grazing management. Furthermore, our projections suggest that without human intervention, ruminant-related emissions would triple over the next eighty years, seriously jeopardizing the achievement of the Paris Agreement targets. These findings advance our understanding of the climate impacts of the ruminant sector from a system perspective, and underscore the urgent

need for rapid and substantial emissions reductions to mitigate climate change. We provided global quantitative evidence for a trade-off between climate mitigation and health outcomes associated with meat reduction. It is worth noting that about 35% of the global population, mainly in the countries of South Asia and Africa, cannot currently afford a healthy diet[35]. In this case, a shift towards healthier diets could paradoxically increase GHG emissions for these developing regions[31], suggesting that ambitious changes towards a healthy diet alone may not be sufficient to meet national GHG reduction commitments.

Under the synergistic scenario, most (71%) of the world's countries could achieve net-zero emissions for ruminant sector while safeguarding human health (Fig. 5b). However, the combined strategies should be carefully tailored to each country's specific context (Fig. 5c). The predominance of supply-side mitigation potential underscores the need to prioritize grazing management (e.g., optimizing grazing intensity and sparing land) and preventing pasture expansion into forests in tropical regions. For Europe, Canada, and South Asia, mitigation efforts should emphasize shifting to lower population growth (e.g., through education and family planning programs), reducing food waste and loss (e.g., enhancing logistics and supply chain management), and increasing production efficiency (e.g., technological innovation and efficient agricultural practices). Moreover, in China and the United States, an integrated approach targeting both demand- and supply-side measures is essential.

Our analysis is subject to several uncertainties. First, due to the limited spatial and temporal coverage of field observations (Fig. S2), we used a modelling approach to estimate land-based emissions over time on a global scale, which represent the largest source of uncertainty for total GHG emissions (Table S1). Moreover, while uncertainties associated with global datasets of key predictors (e.g., background fluxes and grazing intensity) were considered in our analysis (see Methods), reducing the intrinsic uncertainties of these datasets remains important. Other global change drivers, such as fire and extreme weather events, may also influence the results and warrant further investigation. Second, our estimates of climate and health outcomes may be sensitive to some underlying assumptions, particularly the use of a constant global social cost of carbon[36] and generalized diet–mortality relationships (Fig. S13), which may not fully reflect regional variations. Last, our synergistic scenario assumes the simultaneous adoption of all measures; however, real-world implementation may face trade-offs across sectors, temporal delays, and affordability constraints that are not well captured in this analysis. While we addressed or tested the influence of several of these

uncertainties (Supplementary Text), future research should prioritize long-term grazing experiments in underrepresented regions (e.g., high latitudes), integrate localized socioeconomic data, and evaluate policy feasibility to more effectively support global mitigation efforts.

Taken together, our findings provide a systems-level, policy-relevant framework for assessing the climate impacts of the global ruminant sector and identifying plausible GHG mitigation strategies that also safeguard public health. These insights can inform national GHG mitigation efforts towards carbon neutrality and reinforce global initiatives aligned with the United Nations Sustainable Development Goals (SDGs), including ending hunger (SDG 2), promoting health (SDG 3), and combating climate change (SDG 13). We call for a rapid and ambitious transformation of the ruminant sector, alongside unprecedented international cooperation, to align climate and health goals within the limits of planetary boundaries.

Methods

GHG boundary definition and estimation

The ruminant sector encompasses both on-farm and off-farm activities associated with the management, production, and consumption of ruminant livestock, including cattle, sheep, and other domesticated ruminants. The GHG accounting boundary for this sector comprises five main categories (Fig. S1): (1) ongoing grazing land, (2) deforested land attributable to pasture expansion, (3) abandoned agricultural land formerly dedicated to livestock or feed crops, (4) live animals, and (5) animal-based food (e.g., ruminant meat and dairy). Each of these categories includes multiple GHG source and sink processes (Fig. S1).

Specifically, land-based emissions or sinks from grazing, deforested, and abandoned lands include both biogeochemical fluxes (GHG emissions and carbon uptake by plant and soils) and biogeophysical effects (local surface temperatures) from altered albedo and surface energy balance (Fig. S1). Emissions from live animals include enteric fermentation, manure management, and upstream emissions from feed crop production (including land use change). Post-farmgate emissions associated with animal products include those from farm, processing, transportation, packaging, retail distribution and food waste and loss (Fig. S1). We used a data-driven framework that integrates field observations with remote sensing datasets to quantify land-based emissions or sinks for the historical period (1961-2019) and under a future business-as-usual scenario (SSP2; 2020-2100). Emissions from livestock and their products were estimated separately based on unit-specific GHG emission intensities (see Below). All emission estimates are harmonized across spatial and temporal scales and integrated into a systems-level assessment of the sector's net emissions.

Land-based emissions or sinks. *Data collection and response quantification*. We compiled GHG flux values associated with livestock grazing and deforestation for pasture expansion (Fig. S20), by conducting a literature search of peer-reviewed studies published before September 2023 in the Web of Science and China National Knowledge Infrastructure databases, using keywords such as "grazing or land use change" and "greenhouse gas or carbon flux". Additional studies were incorporated from existing meta-analyses to complement our dataset[37]. Studies were included based on the following criteria: (1) We included field-based experiments featuring both control (no-grazing) and grazing treatments with large vertebrate herbivores (e.g., cattle, sheep); (2) For experiments with multiple durations, the longest duration was selected; (3) Only land-use change studies that measured GHG dynamics before and after deforestation for pasture were considered. For each study, we

extracted data for CO_2, CH_4 (in upland and wetland systems), and N_2O, along with ancillary environmental (e.g., temperature, precipitation, plant biomass) and experimental (e.g., duration, replicates and standard deviation) variables. In total, we obtained 3,336 and 515 monthly GHG observations from 195 livestock grazing studies and 27 deforestation studies (Fig. S2), respectively.

We calculated the absolute flux difference between control and treatment groups as a metric to quantify the impacts of grazing and deforestation (Δf; Eq1). CH_4 and N_2O fluxes were converted to CO_2 equivalents using global warming potentials of 34 and 298[38], respectively, and expressed in units of mg CO_2-eq m^{-2} h^{-1}.

$$\Delta f = f_T - f_C \quad (1)$$

Where f_T and f_C represent the mean flux values for the treatment and control groups, respectively. Here, for grazing experiments, ungrazed plots were used as controls; for deforestation experiments, original forest plots were used as controls. The Δf and its variations were quantified using *rma.mv* function in R *metafor* package[39].

Potential predictors and modelling. We used an array of variables as potential predictors of Δf. These variables encompass a wide range of environmental (e.g., background fluxes, climate and soil properties) and experimental (e.g., grazing intensity, duration) factors (Table S3 and S4). Specifically, we used the percentage of aboveground biomass consumed as an indicator of grazing intensity (GI), which is widely used in previous studies[11]. Predictors with seasonal variability, such as temperature and precipitation, were used at a monthly time scale, as we aim to characterize the seasonal dynamics of Δf. We conducted a feature selection procedure based on the Boruta algorithm with 500 iterations implemented in the *Boruta* function[40]. This algorithm identifies important predictors by comparing their relevance to randomized shadow features via random forest and is particularly well-suited for ecological datasets characterized by multicollinearity and complex interactions[40].

After removing unimportant predictors (Table S3 and S4) and outliers, we trained different random forest models for each gas type using the *caret* package[41] to predict Δf (Figs. S4 and S8) and understand the main controls (Table S3 and S4; Fig. S6). A grid-search procedure with tenfold cross-validation was used to determine the optimal hyperparameter combinations, minimizing the cross-validation root mean square error (RMSE). To test for and quantify the potential effect of spatial autocorrelation in the model residuals, we performed a Moran's I test[42] and found that there was no significant spatial autocorrelation in our data. Model performance was assessed on the training data using R^2, which ranged from

0.3 to 0.81 (Table S3 and S4). The best-performing models were then combined with global predictor datasets to estimate Δf of CO_2, CH_4 and N_2O during the grazing season for grazing impacts and on an annual basis for deforestation. Detailed information on these global datasets is provided in Table S5. Given data limitations, the grazing season was approximated based on the length of plant growing period, when forage productivity and quality are high[43,44]. The global gridded dataset of the length of plant growing season was calculated based on the VIIRS global land surface phenology product[45]. The global extent of grazing land and deforestation was derived from the Land-Use Harmonization (LUH2) project[46], which offers consistent and spatially explicit estimates of land-use states and transitions over the studied period. To quantify the impacts of grazing on wetland CH_4 dynamics, we used wetland extent data from Ref[47] for the historical period and from Ref[48] for the future projections.

In our study, the uncertainties in estimated land-based emissions arise from two main sources: the spatial distribution of sample sites and uncertainties in globally gridded data sets, especially for key variables such as background carbon flux and grazing intensity (Fig. S7). We used a bootstrap resampling approach to quantify these uncertainties. Specifically, we performed 100 resampling iterations with replacement and correspondingly developed 100 prediction models for each gas type. For background carbon flux and grazing intensity, we assumed truncated normal distributions and randomly generated 100 samples within their respective uncertainty ranges. The uncertainty in background carbon flux was derived from different dataset sources (Table S5), while the uncertainty in grazing intensity was estimated in this study (Supplementary Text). In addition, uncertainties in temperature and precipitation from different CMIP6 models were included for future projections (Table S5). In total, 10,000 simulations were performed to capture the full range of uncertainty in our final projections (Figs. S5 and S9).

Biophysical impacts. Vegetation cover changes induced by grazing activities, such as forage consumption and deforestation, can alter land-atmosphere energy and water exchanges, thereby influencing land surface temperature (LST). To assess the impact of grazing on LST, we used MODIS satellite data for daytime and nighttime LST and the Normalized Difference Vegetation Index (NDVI) from 2000 to 2020 (Table S5), at a monthly temporal resolution and 0.05° spatial resolution. We first calculated global trends in LST and NDVI during the grazing season over the past two decades. Next, we identified 9,952 grid cells with stable NDVI (e.g., less than 2% variation during the observation period) as controls (Fig. S21a), including 6,445

grids in forested areas and 3,507 in grasslands. For each control grid, we defined a 0.3° × 0.3° moving window centered on the grid and calculated the differences in average trends of NDVI (ΔNDVI) and LST (ΔLST) between the control and surrounding grids. Finally, we derived vegetation-specific relationships between ΔNDVI and ΔLST separately for tropical and temperate regions (Fig. S21b, c).

Overall, we found a negative relationship between ΔNDVI and ΔLST, suggesting that livestock grazing may have a warming effect on the local climate. To test the robustness of this finding, we replaced NDVI with leaf area index and observed similar negative relationships (Figs. S22a, b). We also assessed the effect of grazing on soil temperature using field observations. The results showed that grazing generally increased soil temperatures, and that this warming effect was more pronounced at high grazing intensities (Fig. S22c). It is important to note that satellite-based LST measurements capture only local biogeophysical effects, while non-local impacts on surrounding areas unaffected by land-use change are not accounted for[49], warranting further investigation.

We estimated global grazing-induced changes and their uncertainties in LST from 1961 to 2100 by combining our GI estimates and their uncertainties (Supplementary Text), observationally derived ΔNDVI-ΔLST relationships, and ANPP-NDVI relationships from global observational datasets (Fig. S23). To translate these LST changes into CO_2-equivalent metrics (Fig. S24), we applied the transient climate response to cumulative CO_2 emissions (TCRE) at the grid level (Eq. 2), based on an ensemble mean from 21 CMIP5 models[50].

$$CO_{2_e}^{BGP} = \frac{\Delta°C^{BGP}}{TCRE} \times \frac{1}{A_{Earth}} \times f_{grazing} \qquad (2)$$

Where $\Delta°C^{BGP}$ and $CO_{2_e}^{BGP}$ represent grazing-induced LST changes and their corresponding CO_2-equivalent emissions, respectively. A_{Earth} denotes the total area of the Earth, and $f_{grazing}$ is the proportion of grazed land.

The biophysical effects of deforestation for pasture expansion were quantified on the basis of Ref[50], which provides observational estimates and associated uncertainties of the global biophysical impact of forest change.

Carbon sequestration from abandoned land. In this study, abandoned land associated with ruminant production includes both formerly grazed land and cropland previously used to grow feed crops. Based on LUH2 datasets, we derived the annual global extent of such abandoned land for the period 1961–2100. Specifically, abandoned grazing land was identified by

calculating the year-to-year decline in grazing land fraction, after excluding land transitioned to other uses such as urban expansion or conversion to other types of agriculture. A similar approach was applied to estimate abandoned cropland used for feed production, using a global dataset of crop harvest allocation to animal feed[51]. Carbon sequestration was then estimated by combining the extent of abandoned land with ecosystem carbon sequestration rates (ECSRs). Given the vast area of grazing land globally, ECSRs and the associated uncertainties for abandoned grazing land were derived from 2,965 paired field observations (Fig. S2), distinguishing between pastureland in potential forest regions and rangeland in potential grassland regions (see *EAT-Lancet health and vegan diets* section). For abandoned cropland, ECSRs were obtained from Ref[52]. Additionally, we quantified the biophysical impacts of land abandonment using the same methodology described above.

Emissions from live animals. We estimated GHG emissions from live animals (cattle and sheep) for the period 1961–2100, based on livestock numbers and the corresponding emission intensity per head. Historical livestock population data at the national level were obtained from the FAO production database (https://www.fao.org/faostat/en/#data). Future BAU projections were developed using historical relationships between domestic ruminant meat production and animal populations for each livestock species and country (Fig. S25). These relationships were evaluated using four statistical models, including both linear and non-linear approaches (Fig. S26). The average model performance (R^2) across countries worldwide was 0.62 for cattle and 0.71 for sheep.

Ruminant meat was chosen as the predictor variable, rather than dairy products, because it better reflects livestock population dynamics (Figure S26). Domestic production of ruminant meat was calculated by adjusting national consumption data for imports and exports, using data from the FAO Food Balance Sheets. The contribution of trade to domestic production was assumed to remain constant over time. Future demand for ruminant meat was estimated for each country as described in section *Emissions from animal products*.

Region-specific GHG emissions intensity per head, along with their associated uncertainties, were derived from the Global Livestock Environmental Assessment Model version 3 (GLEAM3)[8], which simulates emissions from biophysical processes within livestock systems based on life cycle assessment. We assumed that national GHG emissions intensity per head remains constant through to 2100. Uncertainties of livestock emissions over 1961–2019 were estimated based on the variations in GHG emissions intensity[8]. For future projections, uncertainties were quantified from 400 combined estimates, generated by pairing

the four production projections with 100 bootstrap samples from the uncertainty range of GHG emissions intensity.

Emissions from animal products. We calculated GHG emissions from animal food consumption (ruminant meat and dairy) for the period 1961-2100 based on per capita demand (gram per person per day), the associated emission intensity per unit of food consumed[1] and population data. Per capita demand and population at the national level from 1961 to 2019 were obtained from the FAO database. In particular, FAO data on food availability only consider food losses and waste (FLW) at the retail and consumer level. Additional FWL at other stages, such as production, storage and processing, were obtained from Ref[53], which has compiled a country-level database assessing FLW across global value chains. FLW per capita for each country was assumed to remain constant over time.

Future ruminant meat demand for each country under the BAU scenario was estimated using a historical relationship between per capita meat consumption (including non-ruminant meat) and per capita GDP for eight economic groups (Fig. S27)[54]. Based on model-averaged national GDP and population projections from SSP2 scenario, taken from Ref[55], we estimated future per capita meat demand for each country using the empirical relationship. Similarly, future national per capital demand for total calorie intake was projected using the same approach. Demand for other foods within 11 major food groups - such as grains, vegetables and fruits, dairy products and eggs - was derived based on the projected demand for meat and total calories, assuming that the composition of foods within each group remains constant until 2100.

Food-related GHG emission intensities were obtained from Ref[1], which provides a comprehensive database of emission intensities and associated uncertainties by gas type derived from meta-analyses of life cycle assessments. In particular, as emissions from deforestation have been estimated separately using a data-driven approach (see above), we have excluded this part from the emission intensities for ruminant meat and dairy calculated using the IPCC Tier method. The variations associated with emission intensity data were used to quantify the overall uncertainty in GHG emissions from animal-sourced products in this study. We assumed that food GHG emission intensities remain constant through to 2100.

Uncertainty propagation. The following equation was used to express the uncertainties of the aggregated total emissions within each category or across different categories and (σ_{total}). The total uncertainty was calculated using the root-sum-square method, assuming that the individual components are independent:

$$\sigma_{total} = \sqrt{\sum_{i=1}^{n} \sigma_i^2} \quad (3)$$

where σ_i represents the standard deviation associated with each emissions component *i*.

Evaluating climate and health impacts of meat reduction

In this study, we defined five scenarios representing different levels of meat consumption reduction, ranging from 10% to 90% relative to the BAU, at 20% intervals (Fig. 3a). In each scenario, the calorie loss from reduced meat intake would be compensated by increased consumption of other food groups, keeping total per capita calorie intake constant. Similar to the method of previous studies[27], we assumed that the relative contribution of individual foods to per capital total caloric intake would remain constant over time.

GHG emissions. For each scenario, we quantified GHG emissions from the ruminant sector in 2020-2100 using the same approach as described for BAU scenario. To cover a wider range of future possibilities, we estimated livestock numbers using two methods. The first method extrapolated from national empirical relationships between livestock numbers and domestic meat demand over the historical period (empirical method; Fig. S26). The second assumed a proportional reduction in livestock numbers in line with the reduction in meat consumption (proportional method). It is important to note that in these scenarios, changes in livestock numbers only affected grazing intensity at the grid level within the on-farm stage. Other variables, including the extent of grazed, deforested and abandoned land, were assumed to remain constant at the BAU level.

Health outcomes. In this study, we assessed the health impact of dietary changes by estimating adult mortality attributable to changes in the prevalence (%) of three BMI-defined weight categories: underweight (BMI < 18.5 kg/m^2), overweight (25 ≤ BMI < 30 kg/m^2), and obesity (BMI ≥ 30 kg/m^2). National-level prevalence data for 2019 were obtained from the World Health Organization[56]. To predict future trends, we developed empirical relationships between the prevalence of each weight category and per capita consumption of six major food groups (excluding food loss and waste) (Table S6), stratified by country income level according to the World Bank classification. We used regularized regression to fit these relationships, based on the *glmnet* function in R[57], which minimizes overfitting in the presence of multicollinearity between variables. Our analysis identified meat consumption as

the most influential factor affecting the prevalence of all three weight categories (Table S6; Fig. S13). We used the projected food consumption under each meat reduction scenario to estimate the future prevalence of each weight category at the national level.

The total number of adult deaths attributable to the three weight categories in each country in 2019 (D_{weight}) was estimated based on their respective hazard ratios (HRs) and the baseline number of deaths among individuals with normal weight ($D_{baseline}$).

$$D_{weight} = D_{underweight} + D_{overweight} + D_{obesity} \quad (4)$$

here $D_{underweight}$, $D_{overweight}$ and $D_{obesity}$ represent the number of deaths in 2019 attributable to underweight, overweight, and obesity, respectively, which were calculated as follows:

$$D_i = D_{baseline} \times (HR_i - 1) \quad (5)$$

$$D_{baseline} = \frac{D_{all}}{HR_{underweight} + HR_{normal} + HR_{overweight} + HR_{obesity}} \quad (6)$$

Where *i* denotes the three weight categories. D_{weight} represents the total number of deaths in 2019, taken from the 2024 Revision of World Population Prospects (WPP). HR_{normal} is the hazard ratio of normal weight, set as 1. The HRs for underweight, overweight, and obesity are 1.32, 1.14, and 1.7, respectively, taken from a meta-analysis of 239 prospective studies[58]. Future national-level deaths associated with each weight category were projected by scaling D_i in proportion to future changes in the estimated prevalence, total population and D_{weight} from the WPP.

Economic impacts. We translated the climate and health impacts of the meat reduction scenario relative to the BAU pathway into monetary terms to assess their economic impact as a percentage of national GDP over the period 2020-2100 (in constant 2020 USD). For climate impacts, we applied a social cost of carbon of $283 per tons of CO_2, as reported in a recent synthesis of 147 studies[36]. For health impacts, we monetized premature mortality using national values of statistical life (VSL)[59], a metric widely used in benefit-cost analyses to value mortality risks[60]. Projections of future GDP were obtained for each country from Ref[55].

***EAT-Lancet* health and vegan diets.** We further examined the economic impacts of a global adoption of the EAT-Lancet healthy or vegan diets. The EAT-Lancet diet is a reference dietary pattern developed by the EAT-Lancet Commission that aims to promote both human health and environmental sustainability[29]. It emphasizes a high intake of plant-based foods, while limiting red meat and processed foods[61]. For each country, we aggregated food demand (in grams per capita per day) according to the EAT–Lancet food group classifications. We then

calculated the energy content (kilocalories per capita per day) for each food category and adjusted the intake levels to align with EAT–Lancet recommendations of 2,500 kcal per capita per day. Ruminant GHG emissions over 2020-2100 under the EAT-Lancet diet scenario were estimated using the same methodology as described for meat reduction scenarios.

The vegan diet, by contrast, consists entirely of plant-based products. Under this scenario, all deforestation and grazing activities on grazing land are halted, allowing these lands to recover and sequester carbon in plant and soils. To estimate the carbon sequestration potential under this scenario, we compiled 2,965 paired carbon observations from 316 grazing exclusion studies for aboveground, root, and soil across global rangeland and pastureland ecosystems (Fig. S2). Using the same spatial modeling approach as for GHG flux estimation (see *Land-based emissions or sinks*), we produced global spatially-explicit annual estimates and associated uncertainties of carbon sequestration rates for each of the three carbon pools of rangeland and pastureland for the next 80 years (Table S2; Figs. S28-S30). For rangelands, sequestration estimates were derived for potential grassland recovery areas, while for pastures, estimates reflected potential forest regrowth areas. The biophysical impacts under vegan scenario and carbon sequestration potential of croplands previously used to grow animal feed were assessed using the same approach as described for the BAU scenario (see *Land-based emissions or sinks*).

We used two complementary approaches to assess mortality induced by the two dietary transitions. The first approach is consistent with that applied in the meat reduction scenarios (described above), relying on modelled global relationships between food consumption and prevalence of the three weight types. However, this method lacks validation with empirical data. The second approach is based on diet-related mortality risks derived from synthesis studies (Ref[29] for the EAT–Lancet diet and Ref[62,63] for the Vegan diet), which provide epidemiologically grounded estimates. Notably, most of the underlying case studies were conducted in high-income countries, which may limit their generalizability to low- and middle-income regions.

In this section, uncertainties were estimated using 200 bootstrap ensembles derived from the two conversion methods described above, combined with 100 bootstrap samples accounting for variation in the social cost of carbon dioxide, GDP projections, and VSL, assuming a 10% coefficient of variation (Figure 2).

We also performed a number of sensitivity analyses to validate the robustness of our conclusions (see Supplementary Text).

Additional measures beyond healthy diet scenarios

We explored six additional mitigation measures from both demand and supply sides, to further reduce global ruminant emissions under the context of *EAT–Lancet* healthy diets. These measures include: low population growth, reduction of FLW, improvement of production efficiency for animal products, zero future deforestation for pasture, optimized grazing intensity, and land sparing for carbon sequestration. We assessed the climate impact of these measures both individually and in combination, resulting in a total of 48 scenarios (Fig. 4a). For each scenario, ruminant GHG emissions over 2020-2100 were estimated using the same method as in the BAU or meat reduction scenarios.

Demand-side strategies. *Low population growth scenario.* We adjusted the BAU population projections of each country to those under the SSP1 scenario, a more optimistic pathway characterized by lower population growth, in order to reduce the overall demand for animal products. The multi-model averaged SSP1 population data for each country were obtained from Ref[55].

FLW reduction. In this measure, per capita food loss and waste (FLW) across the entire value chain were reduced by 50% relative to BAU levels for each country, consistent with the targets set by the United Nations Sustainable Development Goals[32].

Production efficiency improvement. This measure assumed that production efficiency, defined as GHG emissions per unit of food produced, would improve by 40%, based on estimates from Ref[27].

Supply-side strategies. *Zero deforestation.* We assumed that no further deforestation would occur after 2020, thereby eliminating the high per-area GHG emissions associated with land-use change.

Grazing management. In this study, we developed a framework to optimize grazing intensity and spare land for land-based emission reduction and carbon sequestration over 2020-2100 (Fig. S31), while maintaining livestock populations compatible with the EAT-Lancet healthy diet and minimizing disruption to existing production systems. The framework proceeds in the following steps, applied to each grid cell:

First, we identified low-productivity grazing lands as those that meet one of two criteria: (1) optimal grazing intensity (GI_{opt}) less than 5%, or (2) grazing fraction less than 0.1. For these grid cells, we assessed whether removing grazing altogether would result in a net

climate benefit. Specifically, we compared the sum of carbon uptake from spared land (C_{uptake}) and the increased emissions from replacing grazed feed with crop-based feed ($IE_{crop\ feed}$) with baseline GHG emissions under the EAT-Lancet diet (E). The GI_{opt} dataset was derived from a recent observational study[11] and the current livestock fractions in different production systems at regional level were taken from the GLEAM3. If $C_{uptake} + IE_{crop\ feed} < E$, the whole grazing area in that grid was spared (Fig. S31).

For the remaining cells - either high productivity areas or low productivity areas where complete removal was not beneficial (i.e. $C_{uptake} + IE_{crop\ feed} > E$) - we compared GI_{opt} with the required grazing intensity under the EAT-Lancet diet (GI_{EAT}).

- If $GI_{opt} > GI_{EAT}$, the same number of livestock can be supported on a smaller grazing area by increasing GI_{EAT} to GI_{opt} (Supplementary Text), thus conserving land. Based on the optimal grazing hypothesis[11] (Fig. S6b), this adjustment can reduce or even achieve negative emissions (E_{opt}). We only apply it if $C_{uptake} + E_{opt} < E$.
- If $GI_{opt} < GI_{EAT}$, we have reduced GI_{EAT} to GI_{opt} by replacing part of the livestock feed with crop-based alternatives. This adjustment is only applied if $IE_{crop\ feed} + E_{opt} < E$.

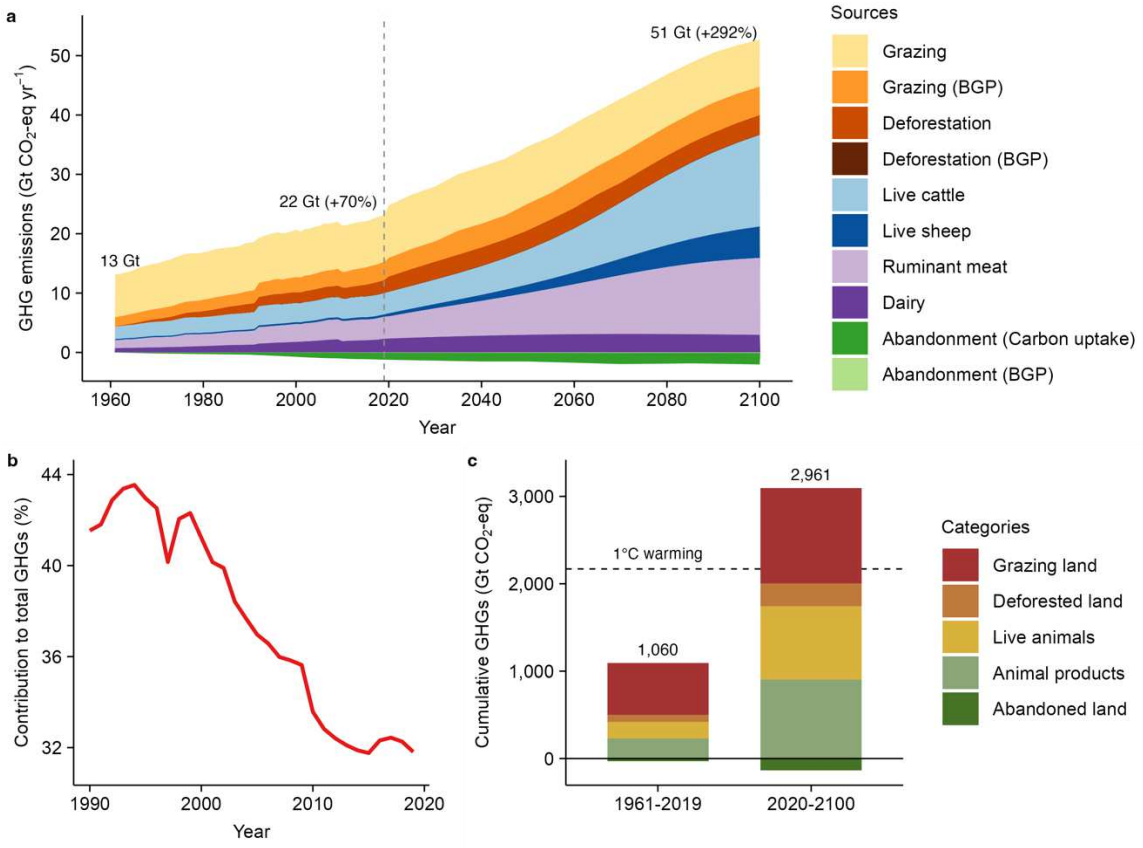

Figure 1. Global GHG emissions from the ruminant sector for 1961-2100. a, Annual GHG emissions from the global ruminant sector, divided into 10 sources in five emission categories, are shown for the historical period (1961-2019) and the projected business-as-usual (BAU) scenario (2020-2100). **b**, Contribution of ruminant emissions to total global anthropogenic GHG emissions derived from the IPCC Sixth Assessment Report. **c**, Cumulative GHG emissions from the global ruminant sector by emission category for the periods 1961-2019 and 2020-2100 under the BAU scenario. Dashed lines in **a** and **c** indicate the year 2019 and the estimated cumulative GHG emissions associated with 1°C global warming, respectively. In **a**, "grazing" refers to these biogeochemical CO_2, CH_4 and N_2O fluxes due to grazing activities, whereas "grazing (BGP)" represents the additional biogeophysical radiative forcing from grazing-altered albedo and surface energy balance; the same "(BGP)" tag is used for deforestation and land abandonment.

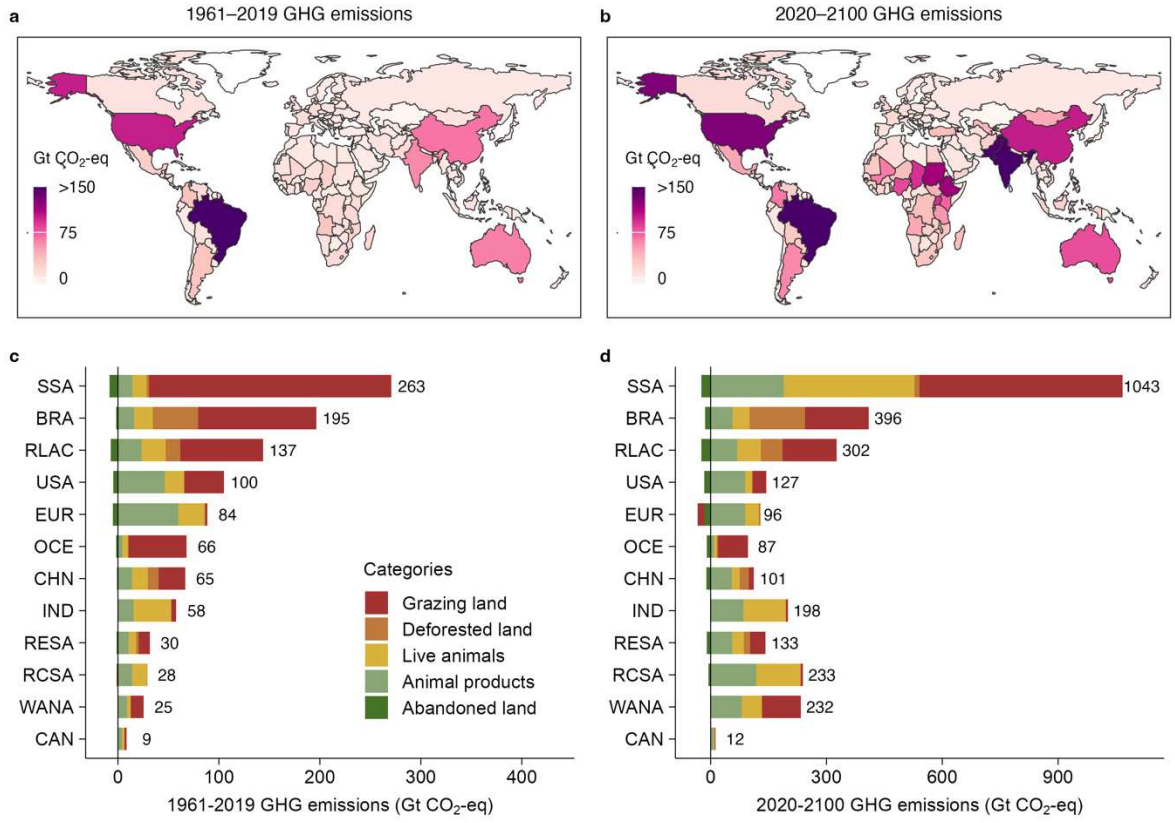

Figure 2. National and regional net GHG emissions from the ruminant sector. a, **b**, Spatial distribution of cumulative net GHG emissions from the ruminant sector across countries for the periods 1961–2019 (**a**) and 2020–2100 under the BAU scenario (**b**). **c**, **d**, Regional cumulative emissions disaggregated by emission category for the periods 1961–2019 (**c**) and 2020–2100 (**d**). SSA, Sub-Saharan Africa; BRA, Brazil; RLAC, Rest of Latin America and the Caribbean; USA, United States; EUR, Europe; OCE, Oceania; CHN, China; IND, India; RESA, Rest of Eastern and South-eastern Asia; RCSA, rest of Central and Southern Asia; WANA, Western Asia and Northern Africa; CAN, Canada.

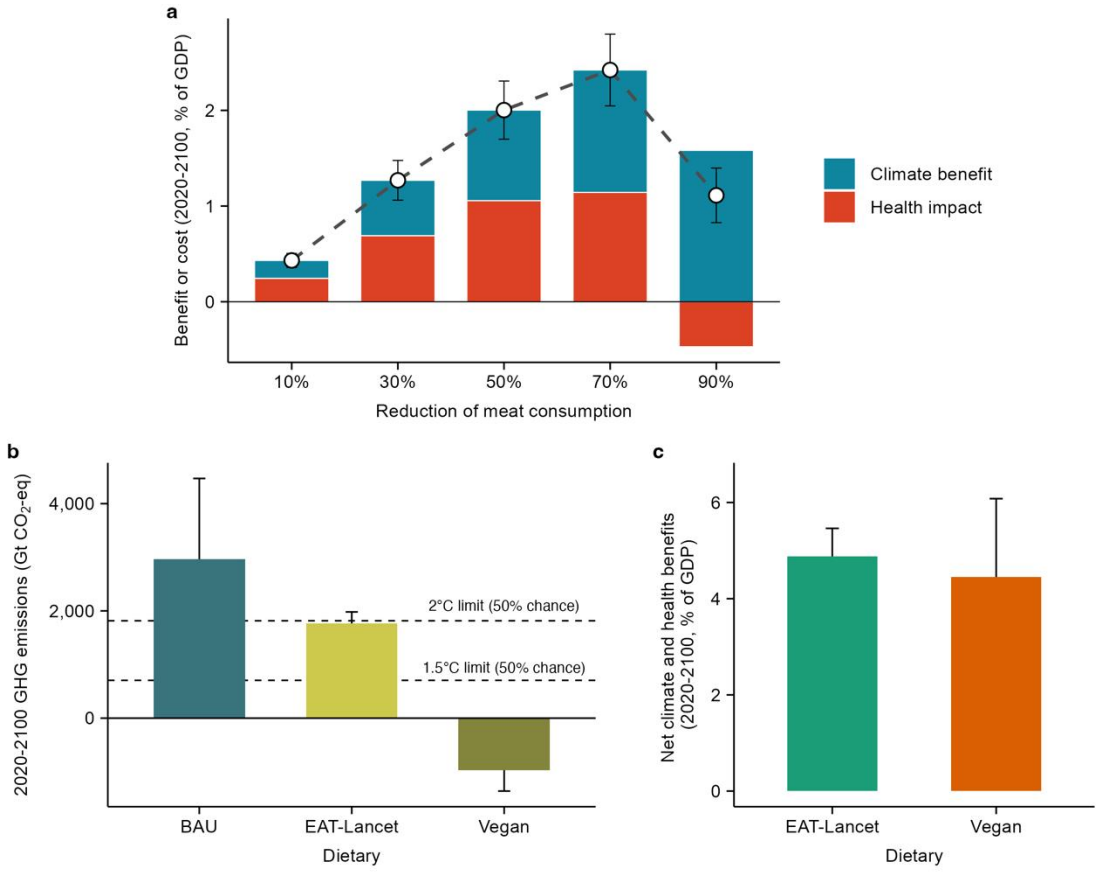

Figure 3. Global economic impacts of reducing meat consumption. a, Economic costs or benefits associated with climate and health impacts of reducing ruminant meat consumption from BAU to different levels. **b**, Projected GHG emissions for 2020-2100 under three dietary scenarios: BAU, EAT-Lancet healthy diet and vegan diet. **c**, Net global climate and health benefits of the EAT-Lancet and vegan diet scenarios compared to the BAU scenario. Points in **a** represent net impacts. The dashed lines in **b** indicate the maximum allowable cumulative emissions over 2020–2100 to limit warming to 1.5 °C and 2 °C with a 50% probability. Error bars represent standard deviations across 200 bootstrap samples (see Methods).

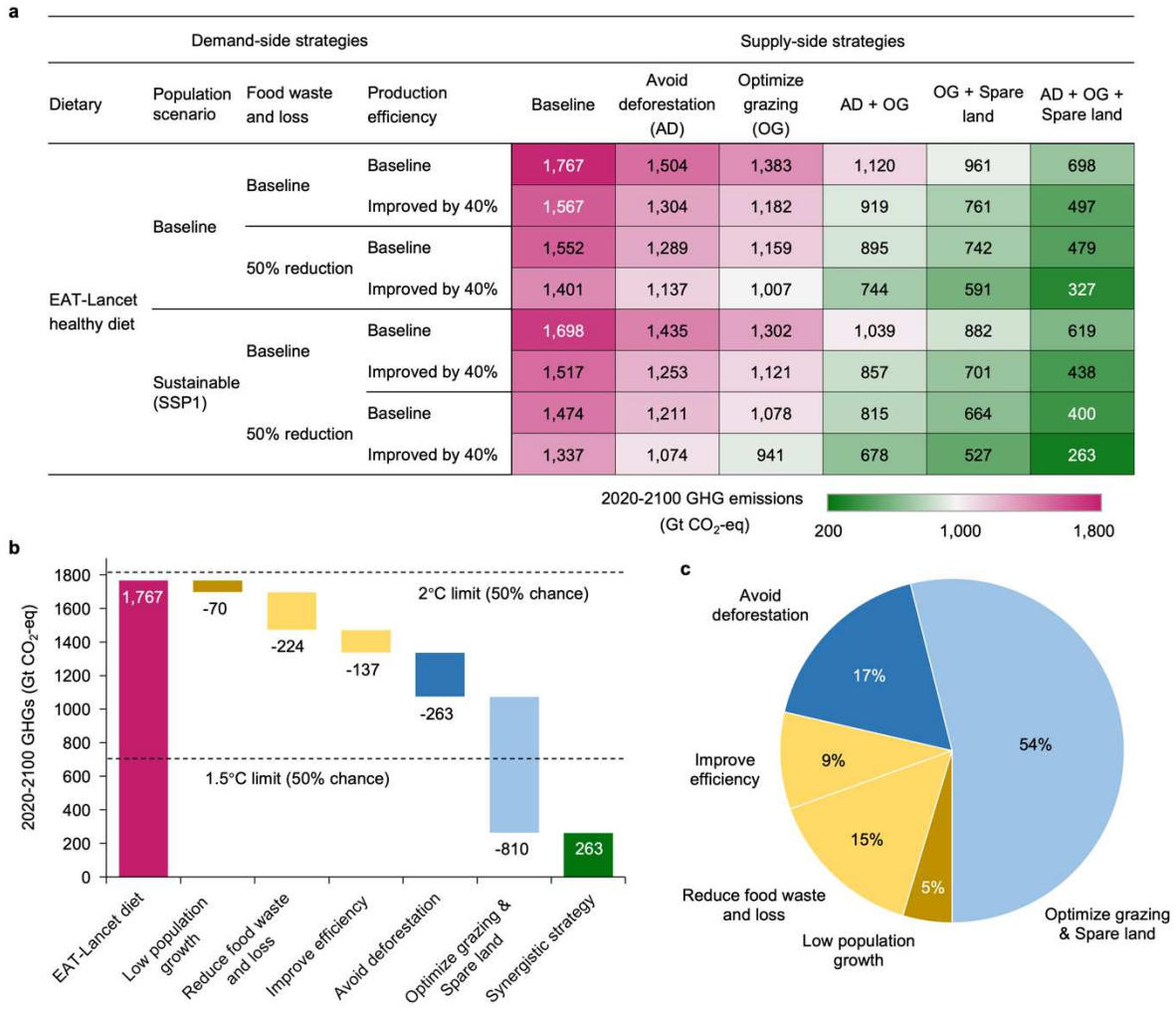

Figure 4. GHG mitigation potential of six strategies under the EAT-Lancet healthy diet scenario. a, Global cumulative GHG emissions from the ruminant sector in 2020-2100 under 48 scenarios derived from combinations of six mitigation strategies. These include: (1) shifting population growth rate towards a more optimistic SSP1 trajectory; (2) halving food loss and waste at the retail and consumer level; (3) improving production efficiency of animal products by 40%; (4) avoiding future deforestation for pasture expansion; (5) optimizing grazing intensity; and (6) conserving land for carbon sequestration under the optimal grazing scenario. **b**, The sequential impact of each strategy on global GHG emissions relative to the healthy diet baseline. The 'synergistic strategy' refers to the simultaneous implementation of all seven measures. **c**, Relative contribution of each strategy to the total GHG reductions achieved under the synergistic scenario.

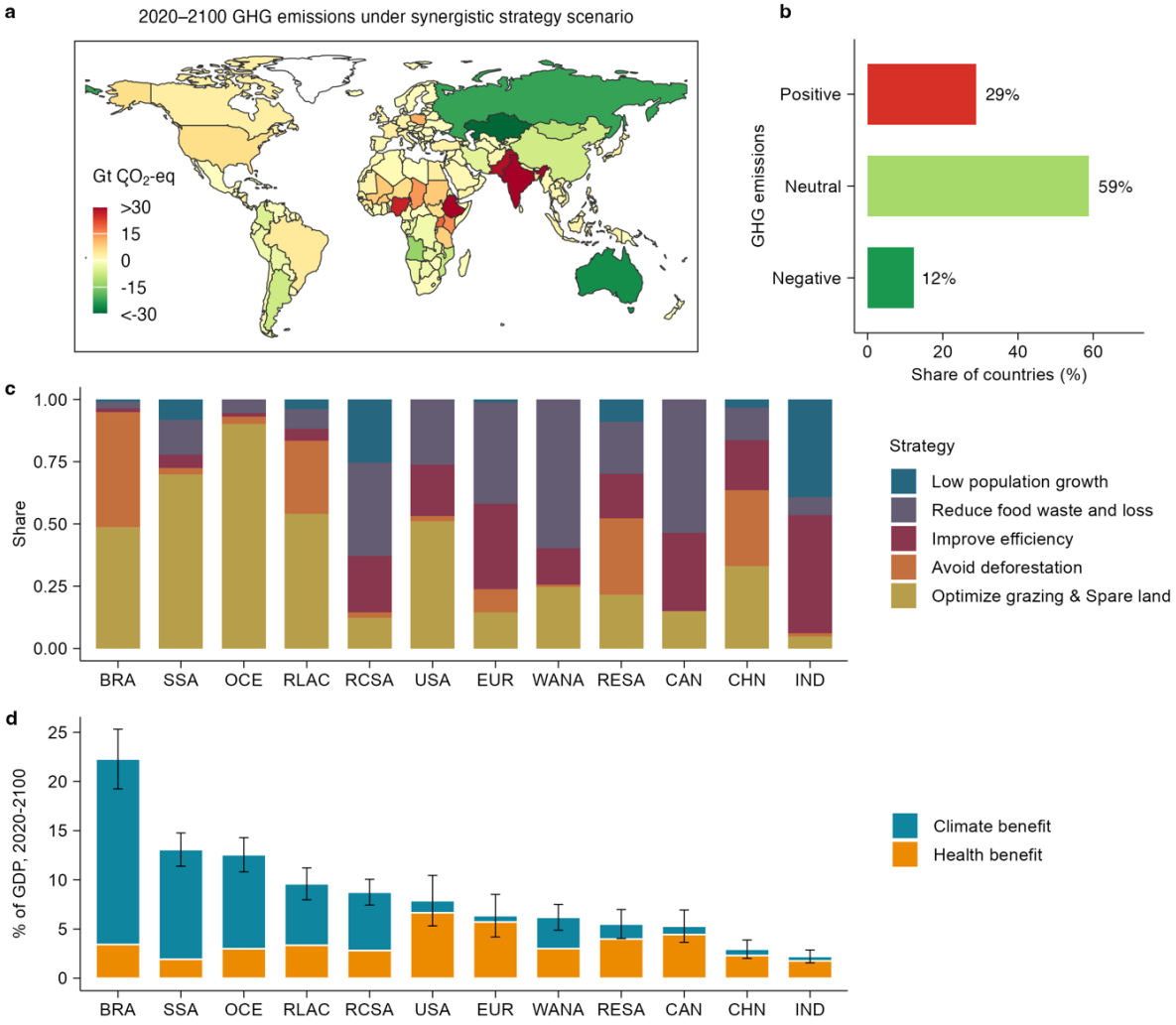

Figure 5. Climate and health co-benefits of implementing synergistic strategies in the ruminant sector. a, Spatial distribution of cumulative ruminant GHG emissions in 2020-2100 under the synergistic mitigation scenario; negative values indicate net carbon uptake from the atmosphere. **b**, Proportion of countries classified by 2020-2100 cumulative emissions as positive (>1 Gt CO_2-eq), neutral (between -1 and 1 Gt CO_2-eq) or negative (<-1 Gt CO_2-eq). **c**, Country and region-level contributions of each strategy to total GHG reductions achieved under the synergistic scenario. **d**, Economic benefits from avoided climate and health damages from BAU to synergistic scenario. Error bars represent standard deviations across 200 bootstrap samples. BRA, Brazil; SSA, Sub-Saharan Africa; OCE, Oceania; RLAC, Rest of Latin America and the Caribbean; RCSA, rest of Central and Southern Asia; USA, United States; EUR, Europe; WANA, Western Asia and Northern Africa; RESA, Rest of Eastern and South-eastern Asia; CAN, Canada; CHN, China; IND, India.

Data and Code availability

The data supporting the findings of this study as well as the code used can be found at https://figshare.com/s/fafc45927da24025ba76

Acknowledgement

This work is supported by the National Science Foundation under Grant No. DEB-2339051.

Author Contributions

S.R. and C.T. conceived the original idea. S.R., Y.C. and Q.H. compiled data from field experiments. X.L, M.W. and Y.X. contributed to the data. S.R. performed the analysis and drafted the manuscript, with input from all authors.

References

1. C. C. Ivanovich, T. Sun, D. R. Gordon, I. B. Ocko, Future warming from global food consumption. Nature Climate Change 13, 297-302 (2023).
2. Y. Wang et al., Risk to rely on soil carbon sequestration to offset global ruminant emissions. Nature Communications 14, 7625 (2023).
3. B. van Oort et al., Ruminating on sustainable food systems in a net-zero world. Nature Sustainability 7, 1225-1234 (2024).
4. J. Poore, T. Nemecek, Reducing food's environmental impacts through producers and consumers. Science 360, 987-992 (2018).
5. A. Parsons, E. Leafe, B. Collett, W. Stiles, The physiology of grass production under grazing. I. Characteristics of leaf and canopy photosynthesis of continuously-grazed swards. Journal of applied ecology, 117-126 (1983).
6. O. J. Schmitz et al., Animals and the zoogeochemistry of the carbon cycle. Science 362, eaar3213 (2018).
7. Z. Zeng et al., Climate mitigation from vegetation biophysical feedbacks during the past three decades. Nature Climate Change 7, 432-436 (2017).
8. C. Opio et al., Greenhouse gas emissions from ruminant supply chains–A global life cycle assessment. (2013).
9. H. Dong, J. D. MacDonald, S. M. Ogle, M. J. S. Sanchez, M. T. Rocha, 2019 Refinement

to the 2006 IPCC Guidelines for National Greenhouse Gas Inventories. Volume 4: Agriculture, Forestry and Other Land Use. IPCC (2019).
10. M. Crippa et al., Food systems are responsible for a third of global anthropogenic GHG emissions. Nature food 2, 198-209 (2021).
11. S. Ren et al., Historical impacts of grazing on carbon stocks and climate mitigation opportunities. Nature Climate Change 14, 380-386 (2024).
12. K. Resare Sahlin et al., An exploration of biodiversity limits to grazing ruminant milk and meat production. Nature sustainability 7, 1160-1170 (2024).
13. M. Herrero et al., Greenhouse gas mitigation potentials in the livestock sector. Nature Climate Change 6, 452-461 (2016).
14. O. J. Schmitz et al., Trophic rewilding can expand natural climate solutions. Nature Climate Change 13, 324-333 (2023).
15. P. Scarborough et al., Vegans, vegetarians, fish-eaters and meat-eaters in the UK show discrepant environmental impacts. Nature Food 4, 565-574 (2023).
16. X. Xu et al., Global greenhouse gas emissions from animal-based foods are twice those of plant-based foods. Nature food 2, 724-732 (2021).
17. H. C. J. Godfray et al., Meat consumption, health, and the environment. Science 361, eaam5324 (2018).
18. L. V. Rasmussen, C. Hall, E. C. Vansant, B. den Braber, R. S. Olesen, Rethinking the approach of a global shift toward plant-based diets. One Earth 4, 1201-1204 (2021).
19. P. Varijakshapanicker et al., Sustainable livestock systems to improve human health, nutrition, and economic status. Animal Frontiers 9, 39-50 (2019).
20. M. N. Hayek et al., Opportunities for carbon sequestration from removing or intensifying pasture-based beef production. Proceedings of the National Academy of Sciences 121, e2405758121 (2024).
21. A. S. Pottinger et al., Pathways to reduce global plastic waste mismanagement and greenhouse gas emissions by 2050. Science 386, 1168-1173 (2024).
22. S. A. Miller, G. Habert, R. J. Myers, J. T. Harvey, Achieving net zero greenhouse gas emissions in the cement industry via value chain mitigation strategies. One Earth 4, 1398-1411 (2021).
23. M. Dai et al., Country-specific net-zero strategies of the pulp and paper industry. Nature 626, 327-334 (2024).
24. H. D. Matthews, N. P. Gillett, P. A. Stott, K. Zickfeld, The proportionality of global warming to cumulative carbon emissions. Nature 459, 829-832 (2009).

25. M. Pathak et al., Climate change 2022 mitigation of climate change: Technical summary. (2022).
26. L. Schuster, P. Taillardat, P. I. Macreadie, M. E. Malerba, Freshwater wetland restoration and conservation are long-term natural climate solutions. Science of The Total Environment 922, 171218 (2024).
27. M. A. Clark et al., Global food system emissions could preclude achieving the 1.5 and 2 C climate change targets. Science 370, 705-708 (2020).
28. M. G. Windisch et al., Hedging our bet on forest permanence for the economic viability of climate targets. Nature Communications 16, 2460 (2025).
29. W. Willett et al., Food in the Anthropocene: the EAT–Lancet Commission on healthy diets from sustainable food systems. The lancet 393, 447-492 (2019).
30. Z. Sun et al., Dietary change in high-income nations alone can lead to substantial double climate dividend. Nature Food 3, 29-37 (2022).
31. Y. Li et al., Reducing climate change impacts from the global food system through diet shifts. Nature Climate Change 14, 943-953 (2024).
32. M. Springmann et al., Options for keeping the food system within environmental limits. Nature 562, 519-525 (2018).
33. B. Bajželj et al., Importance of food-demand management for climate mitigation. Nature Climate Change 4, 924-929 (2014).
34. P. Friedlingstein et al., Global carbon budget 2024. Earth System Science Data Discussions 2024, 1-133 (2024).
35. Unicef, The State of Food Security and Nutrition in the World 2024. (2024).
36. F. C. Moore et al., Synthesis of evidence yields high social cost of carbon due to structural model variation and uncertainties. Proceedings of the National Academy of Sciences 121, e2410733121 (2024).
37. S. Tang et al., Heavy grazing reduces grassland soil greenhouse gas fluxes: A global meta-analysis. Science of the Total Environment 654, 1218-1224 (2019).
38. T. Bao, G. Jia, X. Xu, Weakening greenhouse gas sink of pristine wetlands under warming. Nature Climate Change 13, 462-469 (2023).
39. W. Viechtbauer, Conducting meta-analyses in R with the metafor package. Journal of statistical software 36, 1-48 (2010).
40. M. B. Kursa, A. Jankowski, W. R. Rudnicki, Boruta–a system for feature selection. Fundamenta informaticae 101, 271-285 (2010).
41. M. Kuhn, Building predictive models in R using the caret package. Journal of statistical

838 software 28, 1-26 (2008).
839 42. P. A. Moran, A test for the serial independence of residuals. Biometrika 37, 178-181
840 (1950).
841 43. T. Fetzel, P. Havlik, M. Herrero, K. H. Erb, Seasonality constraints to livestock grazing
842 intensity. Global Change Biology 23, 1636-1647 (2017).
843 44. L. L. Sloat et al., Increasing importance of precipitation variability on global livestock
844 grazing lands. Nature Climate Change 8, 214-218 (2018).
845 45. X. Zhang et al., Generation and evaluation of the VIIRS land surface phenology product.
846 Remote Sensing of Environment 216, 212-229 (2018).
847 46. G. C. Hurtt et al., Harmonization of global land-use change and management for the
848 period 850–2100 (LUH2) for CMIP6. Geoscientific Model Development Discussions
849 2020, 1-65 (2020).
850 47. E. Fluet-Chouinard et al., Extensive global wetland loss over the past three centuries.
851 Nature 614, 281-286 (2023).
852 48. Y. Xi, S. Peng, P. Ciais, Y. Chen, Future impacts of climate change on inland Ramsar
853 wetlands. Nature Climate Change 11, 45-51 (2021).
854 49. J. Winckler, Q. Lejeune, C. H. Reick, J. Pongratz, Nonlocal effects dominate the global
855 mean surface temperature response to the biogeophysical effects of deforestation.
856 Geophysical Research Letters 46, 745-755 (2019).
857 50. M. G. Windisch, E. L. Davin, S. I. Seneviratne, Prioritizing forestation based on
858 biogeochemical and local biogeophysical impacts. Nature Climate Change 11, 867-871
859 (2021).
860 51. D. K. Ray et al., Crop harvests for direct food use insufficient to meet the UN's food
861 security goal. Nature Food 3, 367-374 (2022).
862 52. M. N. Hayek, H. Harwatt, W. J. Ripple, N. D. Mueller, The carbon opportunity cost of
863 animal-sourced food production on land. Nature Sustainability 4, 21-24 (2021).
864 53. A. Gatto, M. Chepeliev, Global food loss and waste estimates show increasing nutritional
865 and environmental pressures. Nature Food 5, 136-147 (2024).
866 54. D. Tilman, M. Clark, Global diets link environmental sustainability and human health.
867 Nature 515, 518-522 (2014).
868 55. K. Riahi et al., The Shared Socioeconomic Pathways and their energy, land use, and
869 greenhouse gas emissions implications: An overview. Global environmental change 42,
870 153-168 (2017).
871 56. N. H. Phelps et al., Worldwide trends in underweight and obesity from 1990 to 2022: a

pooled analysis of 3663 population-representative studies with 222 million children, adolescents, and adults. The Lancet 403, 1027-1050 (2024).
57. J. Friedman et al., Package 'glmnet'. CRAN R Repositary 595 (2021).
58. E. Di Angelantonio et al., Body-mass index and all-cause mortality: individual-participant-data meta-analysis of 239 prospective studies in four continents. The lancet 388, 776-786 (2016).
59. W. K. Viscusi, Pricing the global health risks of the COVID-19 pandemic. Journal of Risk and Uncertainty 61, 101-128 (2020).
60. Y. Sun et al., Global supply chains amplify economic costs of future extreme heat risk. Nature 627, 797-804 (2024).
61. Z. Sun, L. Scherer, Q. Zhang, P. Behrens, Adoption of plant-based diets across Europe can improve food resilience against the Russia–Ukraine conflict. Nature Food 3, 905-910 (2022).
62. P. N. Appleby, T. J. Key, The long-term health of vegetarians and vegans. Proceedings of the Nutrition Society 75, 287-293 (2016).
63. M. Dinu, R. Abbate, G. F. Gensini, A. Casini, F. Sofi, Vegetarian, vegan diets and multiple health outcomes: A systematic review with meta-analysis of observational studies. Critical reviews in food science and nutrition 57, 3640-3649 (2017).

Supplementary Files

This is a list of supplementary files associated with this preprint. Click to download.

- Supplementary.docx